**Theranostic Pretargeted Radioimmunotherapy of Internalizing Solid Tumor Antigens in Human Tumor Xenografts in Mice: Curative Treatment of HER2-Positive Breast Carcinoma**

Sarah M. Cheal[1,2], Hong Xu[3], Hong-fen Guo[3], Mitesh Patel[2], Blesida Punzalan[1,2], Edward K. Fung[4], Sang-gyu Lee[4], Meghan Bell[2], Manisha Singh[1], Achim A. Jungbluth[5], Pat B. Zanzonico[4], Alessandra Piersigilli[6], *Steven M. Larson[1,2], *Nai-Kong V. Cheung[1,3]

1. Molecular Pharmacology Program, Memorial Sloan Kettering Cancer Center, New York, NY 10065, USA
2. Department of Radiology, Memorial Sloan Kettering Cancer Center, New York, NY 10065, USA
3. Department of Pediatrics, Memorial Sloan Kettering Cancer Center, New York, NY 10065, USA
4. Department of Medical Physics, Memorial Sloan Kettering Cancer Center, New York, NY 10065, USA
5. Department of Pathology, Memorial Sloan Kettering Cancer Center, New York, NY 10065, USA
6.Tri-Institutional Laboratory of Comparative Pathology, Memorial Sloan Kettering Cancer Center, Weill Cornell Medicine, and The Rockefeller University, New York, NY 10065, USA

*S.M.L and NK.V.C are Co-PIs on this project.

Corresponding author: S.M.L. (Phone: 646-888-2212; Fax: 646-717-3263; Email: larsons@mskcc.org)

**Supplementary Files**

**Table of Contents**

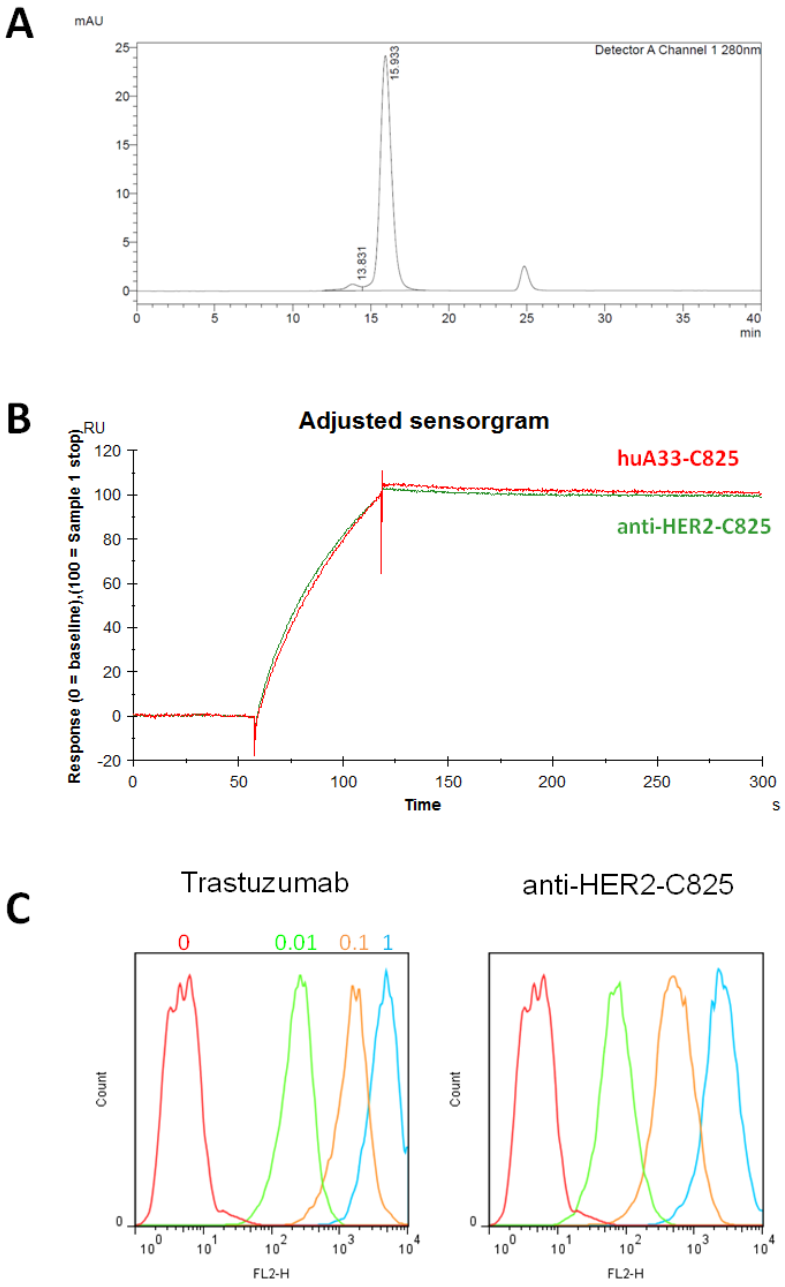


**Figure S1.** *In vitro* characterization of anti-HER2-C825 BsAb. (A) Biochemical purity of HER2-C825 by SE-HPLC chromatogram (UV 280 nm). The major peak (15.933 min) is the fully paired BsAb with an approximate molecular weight of 210 kDa (>96% integrated area under the curve); 25 min is the salt buffer peak. (B) Biacore sensorgrams of BsAbs binding to BSA-(Y)-DOTA-Bn. (C) FACS histograms of antibodies binding to the HER2(+) breast cancer cell line AU565. The top of the left histogram recorded the concentrations of antibodies (μg/$10^6$ cells), and Rituxan was used as negative control (MFI set at 5).

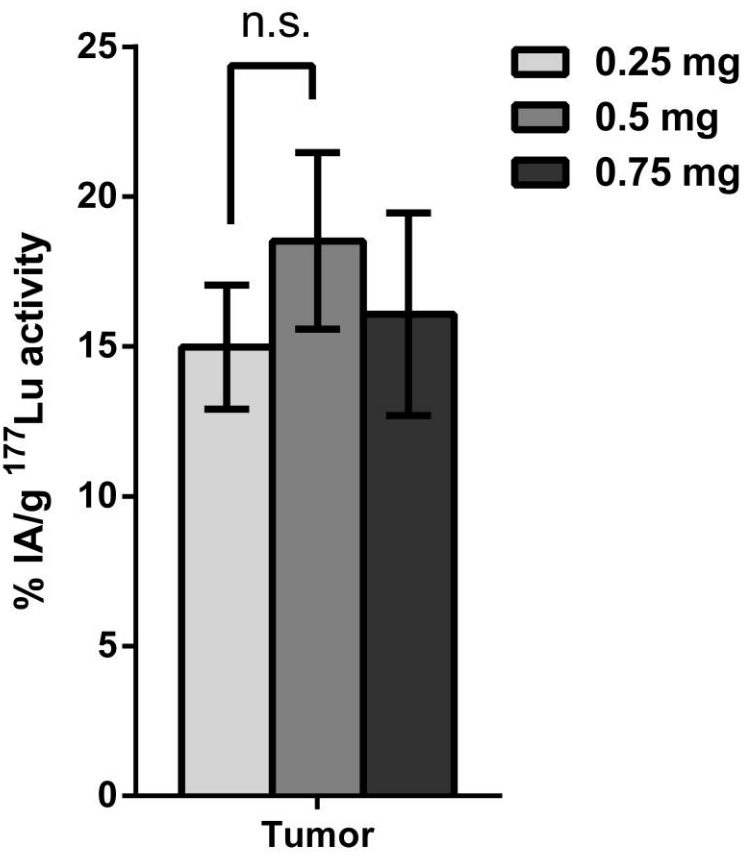


**Figure S2.** *Ex vivo* biodistribution studies of $^{177}$Lu activity in various tissues for optimization of BsAb for anti-HER2-DOTA-PRIT with $^{177}$Lu-DOTA-Bn (5.5-5.6 MBq; ~30 pmol) in groups of nude mice bearing s.c. BT-474 tumors ($n$ = 4/group). No clearing agent step was given. $^{177}$Lu activity uptake (as %IA/g; mean ± SD) at 24 h p.i. in tumor following anti-HER2-DOTA-PRIT including various doses of BsAb (0.25, 0.50, or 0.75 mg BsAb/mouse; 1.19-3.57 nmol/mouse) was determined. No significant (n.s.) difference ($P$ > 0.05) was seen in tumor uptake of $^{177}$Lu activity between groups given either 0.25 mg BsAb/mouse or 0.50 mg BsAb/mouse, suggesting that 0.25 mg BsAb/mouse was optimal.

| Tissues | 0 µg saline ($n$ = 4) | 7.5% w/w 18.75 µg ($n$ = 4) | 14% w/w 37.5 µg ($n$ = 4) | 28% w/w 70 µg ($n$ = 4) |
|---|---|---|---|---|
| Blood | 4.95 ± 1.17 | 1.03 ± 0.58 | 0.52 ± 0.08 | 0.27 ± 0.08 |
| Heart | 1.14 ± 0.29 | 0.45 ± 0.27 | 0.15 ± 0.03 | 0.11 ± 0.04 |
| Lungs | 2.11 ± 0.45 | 0.46 ± 0.23 | 0.35 ± 0.05 | 0.25 ± 0.05 |
| Liver | 1.85 ± 0.30 | 0.49 ± 0.25 | 0.46 ± 0.04 | 0.33 ± 0.02 |
| Spleen | 1.00 ± 0.21 | 0.58 ± 0.14 | 0.69 ± 0.20 | 0.73 ± 0.18 |
| Stomach | 0.34 ± 0.09 | 0.12 ± 0.03 | 0.14 ± 0.03 | 0.05 ± 0.02 |
| Small Int. | 0.58 ± 0.12 | 0.22 ± 0.12 | 0.17 ± 0.07 | 0.07 ± 0.01 |
| Large Int. | 0.58 ± 0.12 | 0.24 ± 0.08 | 0.36 ± 0.16 | 0.19 ± 0.04 |
| Kidneys | 2.31 ± 0.52 | 0.75 ± 0.46 | 0.78 ± 0.09 | 0.75 ± 0.08 |
| Muscle | 0.38 ± 0.09 | 0.11 ± 0.03 | 0.08 ± 0.02 | 0.08 ± 0.02 |
| Bone | 0.39 ± 0.16 | 0.09 ± 0.07 | 0.04 ± 0.01 | 0.11 ± 0.16 |
| *Tumor* | *19.94 ± 3.54* | *7.26 ± 0.55* | *6.76 ± 2.39* | *6.98 ± 3.15* |
| *Tumor size (g)* | *0.082 ± 0.021* | *0.122 ± 0.020* | *0.082 ± 0.023* | *0.095 ± 0.035* |
| *Tumor-to-tissue ratios* | | | | |
| Blood | 4.0 ± 1.2 | 7.1 ± 4.1 | 13.1 ± 5.1 | 25.6 ± 13.9 |
| Heart | 17.5 ± 5.4 | 16.0 ± 9.6 | 45.1 ± 18.9 | 63.5 ± 35.2 |
| Lungs | 9.5 ± 2.6 | 15.8 ± 7.9 | 19.6 ± 7.4 | 28.5 ± 14.3 |
| Liver | 10.8 ± 2.6 | 15.0 ± 7.8 | 14.6 ± 5.3 | 21.2 ± 9.7 |
| Spleen | 19.9 ± 5.5 | 12.6 ± 3.3 | 9.8 ± 4.4 | 9.6 ± 4.9 |
| Stomach | 59.1 ± 18.8 | 59.2 ± 17.0 | 50.1 ± 20.7 | 133.0 ± 76.7 |
| Small Int. | 34.5 ± 9.3 | 33.7 ± 19.2 | 39.8 ± 21.2 | 99.7 ± 47.9 |
| Large Int. | 34.4 ± 9.3 | 29.9 ± 10.7 | 18.9 ± 10.9 | 37.7 ± 18.5 |
| Kidneys | 8.6 ± 2.5 | 9.7 ± 6.0 | 8.7 ± 3.2 | 9.4 ± 4.3 |
| Muscle | 52.1 ± 15.2 | 67.5 ± 20.1 | 84.5 ± 37.6 | 84.6 ± 45.2 |
| Bone | 50.8 ± 22.7 | 80.6 ± 61.9 | 159.0 ± 66.7 | 63.5 ± 97.0 |

**Table S1.** *Ex vivo* biodistribution studies of $^{177}$Lu activity in various tissues for optimization of CA for anti-HER2-DOTA-PRIT with $^{177}$Lu-DOTA-Bn in nude mice bearing s.c. BT-474 tumors. Groups of HER2(+) tumor-bearing mice ($n$ = 4/group) were injected with 0.25 mg (1.19 nmol) of anti-HER2-C825 [$t$ = -28 h], followed by CA (0-28% (*w*/*w*)/mouse with respect to administered anti-HER2-C825 BsAb mass of 0.25 mg/mouse; 0-70 µg/mouse; 0-0.14 nmol of dextran; 0-8.5 nmol of (Y)-DOTA-Bn) [$t$ = -4 h], and 5.5-5.6 MBq (~30 pmol) of $^{177}$Lu-DOTA-Bn [$t$ = 0 h], and sacrificed at 24 h p.i. for biodistribution in tumor and normal tissue. $^{177}$Lu activity concentration data is presented as %IA/g (mean ± SD). Tumor sizes are presented as gram (g) (mean ± SD).

| Tumor type | BT-474 HER2(+) | BT-474 HER2(+) | MDA-MB-468 HER2(-) | BT-474 HER2(+) |
|---|---|---|---|---|
| Tissues | PRIT + CA 62.5 μg 0.125 nmol of dextran; 7.63 nmol of (Y)-DOTA-Bn (*n* = 5) | PRIT + no CA (*n* = 4) | PRIT + no CA (*n* = 5) | no PRIT, only $^{177}$Lu-DOTA-Bn[a] (*n* = 2) |
| Blood | 0.28 ± 0.09 | 4.95 ± 0.58 | 6.59 ± 1.31 | 0.002 ± 0.00 |
| Heart | 0.07 ± 0.02 | 1.14 ± 0.14 | 1.78 ± 0.29 | n.d |
| Lungs | 0.20 ± 0.05 | 2.11 ± 0.23 | 2.44 ± 0.42 | n.d. |
| Liver | 0.27 ± 0.07 | 1.85 ± 0.15 | 2.69 ± 0.35 | 0.04 ± 0.01 |
| Spleen | 0.60 ± 0.21 | 1.00 ± 0.11 | 1.06 ± 0.16 | 0.02 ± 0.00 |
| Stomach | 0.06 ± 0.01 | 0.34 ± 0.04 | 0.27 ± 0.04 | n.d. |
| Small Int. | 0.05 ± 0.01 | 0.58 ± 0.06 | 0.61 ± 0.11 | n.d. |
| Large Int. | 0.18 ± 0.01 | 0.58 ± 0.06 | 0.35 ± 0.06 | n.d. |
| Kidneys | 0.73 ± 0.05 | 2.31 ± 0.26 | 2.39 ± 0.54 | 0.38 ± 0.01 |
| Muscle | 0.06 ± 0.01 | 0.38 ± 0.04 | 0.50 ± 0.14 | n.d. |
| Bone | 0.04 ± 0.01 | 0.39 ± 0.08 | 0.62 ± 0.17 | n.d. |
| *Tumor* | *7.58 ± 0.78* | *19.94 ± 1.77* | *2.75 ± 0.17* | *0.07 ± 0.01* |

[a]no BsAb or CA injected, only ~16.8 MBq of $^{177}$Lu-DOTA-Bn (90 pmol)

**Table S2.** Biodistribution data at 24 h p.i. of $^{177}$Lu-DOTA-Bn (~5.6 MBq, 30 pmol, unless otherwise noted) designed to demonstrate HER2(+) tumor-specific targeting in mice bearing either s.c. HER2(+) (BT-474) or s.c. HER2(-) (MDA-MB-468) tumors. In addition, biodistribution data is provided for 24 h p.i. of $^{177}$Lu-DOTA-Bn only into mice bearing BT-474 HER2(+) tumors. All tumors ranged from 100-200 mg *ex vivo*. n.d. = not determined; Int. = intestine. Data is presented as %IA/g (mean ± SEM).

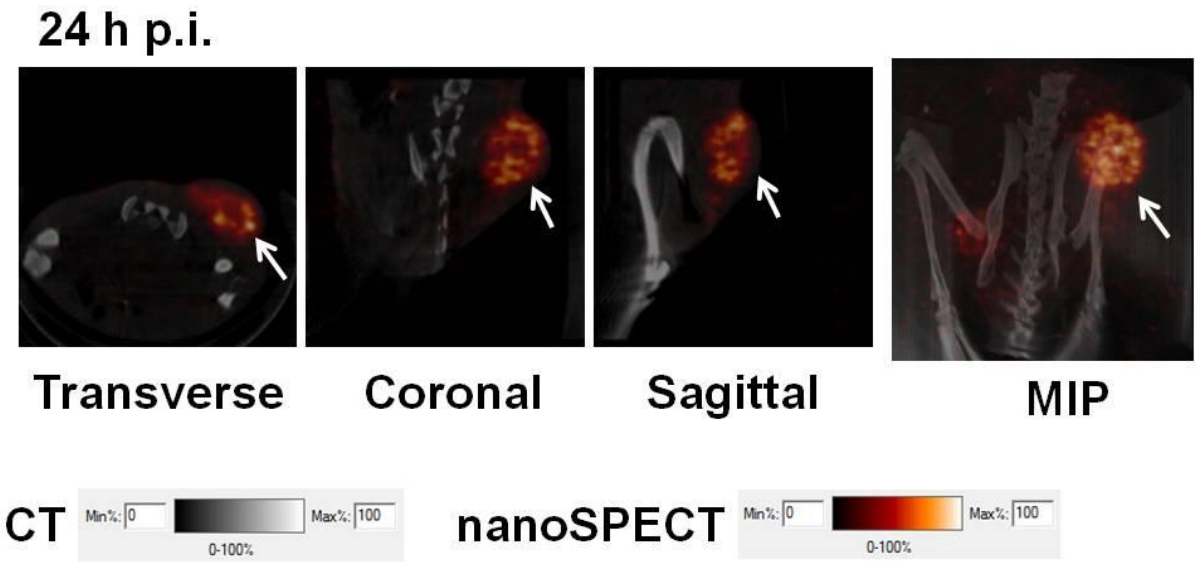


**Figure S3.** Representative SPECT/CT images of a s.c. BT-474 tumor-bearing mouse (216 $mm^3$ by external caliper measurement) 24 h p.i. of anti-HER2-DOTA-PRIT pretargeted $^{177}$Lu-DOTA-Bn (55.5 MBq, ~300 pmol). The imaging field of view was limited to the caudal half of the animal (midline to tail) to center of tumor (*white arrow*). Immediately after imaging, the mouse was euthanized and the activity concentrations in tumor was determined by *ex vivo* biodistribution (as %IA/g, decay-corrected) to be 6.06 (for $n$ = 3/5.53 ± 0.27 %IA/g). MIP = maximum intensity projection.

| Tissues | 1.0 h ($n$ = 5) | 2.5 h ($n$ = 5) | 24 h ($n$ = 5) | 96 h ($n$ = 5) | 336 h ($n$ = 4) |
|---|---|---|---|---|---|
| Blood | 0.62 ± 0.06 | 0.41 ± 0.04 | 0.28 ± 0.09 | 0.04 ± 0.00 | 0.002 ± 0.00 |
| Heart | 0.17 ± 0.03 | 0.13 ± 0.02 | 0.07 ± 0.02 | 0.05 ± 0.01 | 0.01 ± 0.00 |
| Lungs | 0.40 ± 0.05 | 0.37 ± 0.03 | 0.20 ± 0.05 | 0.07 ± 0.01 | 0.01 ± 0.00 |
| Liver | 0.76 ± 0.06 | 0.39 ± 0.04 | 0.27 ± 0.07 | 0.23 ± 0.04 | 0.09 ± 0.02 |
| Spleen | 0.15 ± 0.02 | 0.33 ± 0.03 | 0.60 ± 0.21 | 0.18 ± 0.02 | 0.09 ± 0.02 |
| Stomach | 0.37 ± 0.09 | 0.21 ± 0.07 | 0.06 ± 0.01 | 0.04 ± 0.01 | 0.01 ± 0.00 |
| Small Int. | 1.11 ± 0.27 | 0.47 ± 0.16 | 0.05 ± 0.01 | 0.05 ± 0.01 | 0.003 ± 0.00 |
| Large Int. | 2.22 ± 0.37 | 3.18 ± 0.52 | 0.18 ± 0.01 | 0.07 ± 0.01 | 0.004 ± 0.00 |
| Kidneys | 1.17 ± 0.02 | 0.95 ± 0.05 | 0.73 ± 0.05 | 0.27 ± 0.03 | 0.08 ± 0.01 |
| Muscle | 0.19 ± 0.01 | 0.19 ± 0.04 | 0.06 ± 0.01 | 0.10 ± 0.03 | 0.01 ± 0.00 |
| Bone | 0.18 ± 0.03 | 0.13 ± 0.01 | 0.04 ± 0.01 | 0.38 ± 0.09 | 0.03 ± 0.01 |
| *Tumor* | *6.65 ± 0.46* | *4.95 ± 0.34* | *7.58 ± 0.78* | *2.29 ± 0.41* | *0.32 ± 0.06* |
| *Tumor size (g)* | *0.112 ± 0.062* | *0.135 ± 0.040* | *0.182 ± 0.094* | *0.151 ± 0.104* | *0.183 ± 0.078* |
| *Tumor-to-tissue ratios* | | | | | |
| Blood | 10.7 ± 1.3 | 12.1 ± 1.5 | 26.7 ± 9.0 | 63.6 ± 12.2 | 160.8 ± 30.3 |
| Heart | 38.7 ± 6.7 | 37.5 ± 5.2 | 105.3 ± 27.7 | 42.4 ± 10.3 | 37.8 ± 7.7 |
| Lungs | 16.6 ± 2.3 | 13.5 ± 1.6 | 38.7 ± 10.0 | 34.7 ± 8.8 | 29.2 ± 8.2 |
| Liver | 8.7 ± 0.9 | 12.6 ± 1.6 | 28.3 ± 8.3 | 10.1 ± 2.6 | 3.7 ± 1.0 |
| Spleen | 44.9 ± 6.3 | 14.9 ± 1.8 | 12.6 ± 4.5 | 12.9 ± 2.9 | 3.5 ± 0.9 |
| Stomach | 17.8 ± 4.6 | 23.6 ± 7.7 | 122.3 ± 17.1 | 57.3 ± 13.7 | 51.4 ± 12.4 |
| Small Int. | 6.0 ± 1.5 | 10.6 ± 3.7 | 140.4 ± 22.8 | 44.0 ± 12.6 | 116.9 ± 30.0 |
| Large Int. | 3.0 ± 0.5 | 01.6 ± 0.3 | 41.7 ± 5.4 | 31.8 ± 8.6 | 75.6 ± 26.4 |
| Kidneys | 5.7 ± 0.5 | 5.2 ± 0.5 | 10.4 ± 1.3 | 8.4 ± 1.7 | 3.8 ± 0.9 |
| Muscle | 35.7 ± 3.6 | 25.8 ± 5.1 | 118.5 ± 26.8 | 22.5 ± 8.7 | 64.3 ± 18.4 |
| Bone | 37.3 ± 6.0 | 37.5 ± 4.3 | 189.6 ± 46.7 | 6.0 ± 1.7 | 10.0 ± 3.6 |

**Table S3.** $^{177}$Lu activity data determined using *ex vivo* biodistribution from groups of nude mice bearing s.c. BT-474 tumors at each time indicated p.i. (from 1-336 h) is presented as %IA/g (mean ± SEM). These data are also shown in Figure 3 and were used for dosimetry calculations (Table 2).

| Tissues | PRIT + CA[a] ~30 pmol ($n$ = 5) | PRIT + CA[b] ~300 pmol ($n$ = 3) |
|---|---|---|
| Blood | 0.28 ± 0.09 | 0.29 ± 0.05 |
| Heart | 0.07 ± 0.02 | 0.11 ± 0.02 |
| Lungs | 0.20 ± 0.05 | 0.20 ± 0.02 |
| Liver | 0.27 ± 0.07 | 0.33 ± 0.04 |
| Spleen | 0.60 ± 0.21 | 0.22 ± 0.07 |
| Stomach | 0.06 ± 0.01 | 0.04 ± 0.01 |
| Small Int. | 0.05 ± 0.01 | 0.05 ± 0.01 |
| Large Int. | 0.18 ± 0.01 | 0.20 ± 0.11 |
| Kidneys | 0.73 ± 0.05 | 0.56 ± 0.08 |
| Muscle | 0.06 ± 0.01 | 0.04 ± 0.01 |
| Bone | 0.04 ± 0.01 | 0.04 ± 0.01 |
| *Tumor* | *7.58 ± 0.78* | *5.53 ± 0.27* |

[a]0.25 mg of anti-HER2-C825, 62.5 µg (25% (w/w)) CA, and ~5.6 MBq of $^{177}$Lu-DOTA-Bn
[b]0.25 mg of anti-HER2-C825, 62.5 µg (25% (w/w)) CA, and 55.5 MBq of $^{177}$Lu-DOTA-Bn

**Table S4.** $^{177}$Lu activity data determined using *ex vivo* biodistribution from groups of nude mice bearing s.c. BT-474 tumors at 24 h p.i. of either 0.25 mg of anti-HER2-C825, 62.5 µg (25% (w/w)) CA, and ~5.6 MBq of $^{177}$Lu-DOTA-Bn (30 pmol) or 0.25 mg of anti-HER2-C825, 62.5 µg (25% (w/w)) CA, and 55.5 MBq of $^{177}$Lu-DOTA-Bn (300 pmol).

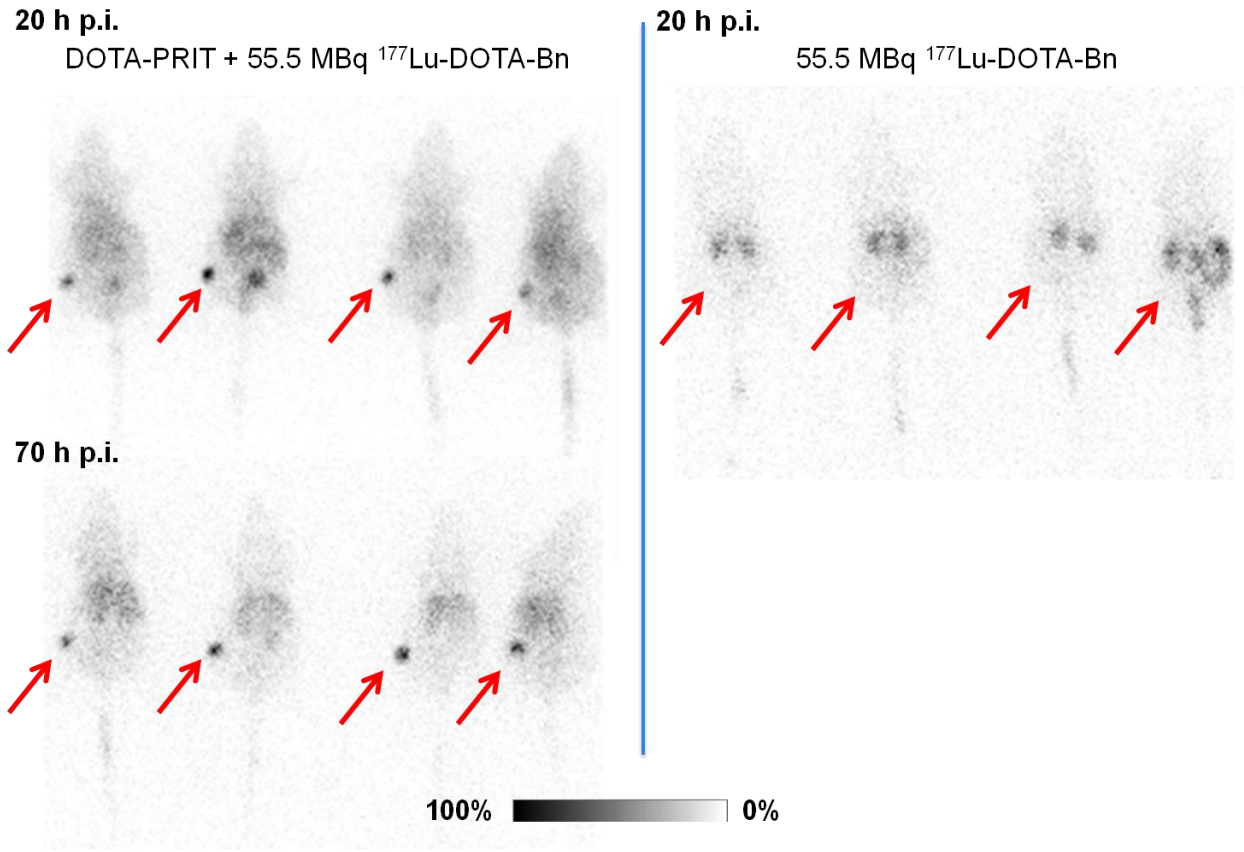


**Figure S4.** Theranostic anti-HER2-DOTA-PRIT + $^{177}$Lu-DOTA-Bn. Planar scintigraphy of groups of mice bearing s.c. BT-474 xenografts (*red arrows*; palpable-30 mm$^3$) undergoing either anti-HER2-DOTA-PRIT + $^{177}$Lu-DOTA-Bn (*left images*) or treatment with non-targeted $^{177}$Lu-DOTA-Bn (*right images*). Pretargeting-specific tumor uptake of $^{177}$Lu activity was evident, while mice administered 55.5 MBq of $^{177}$Lu-DOTA-Bn showed uptake primarily in kidney, consistent with renal clearance of $^{177}$Lu-DOTA-Bn. All images are presented on the same scale.

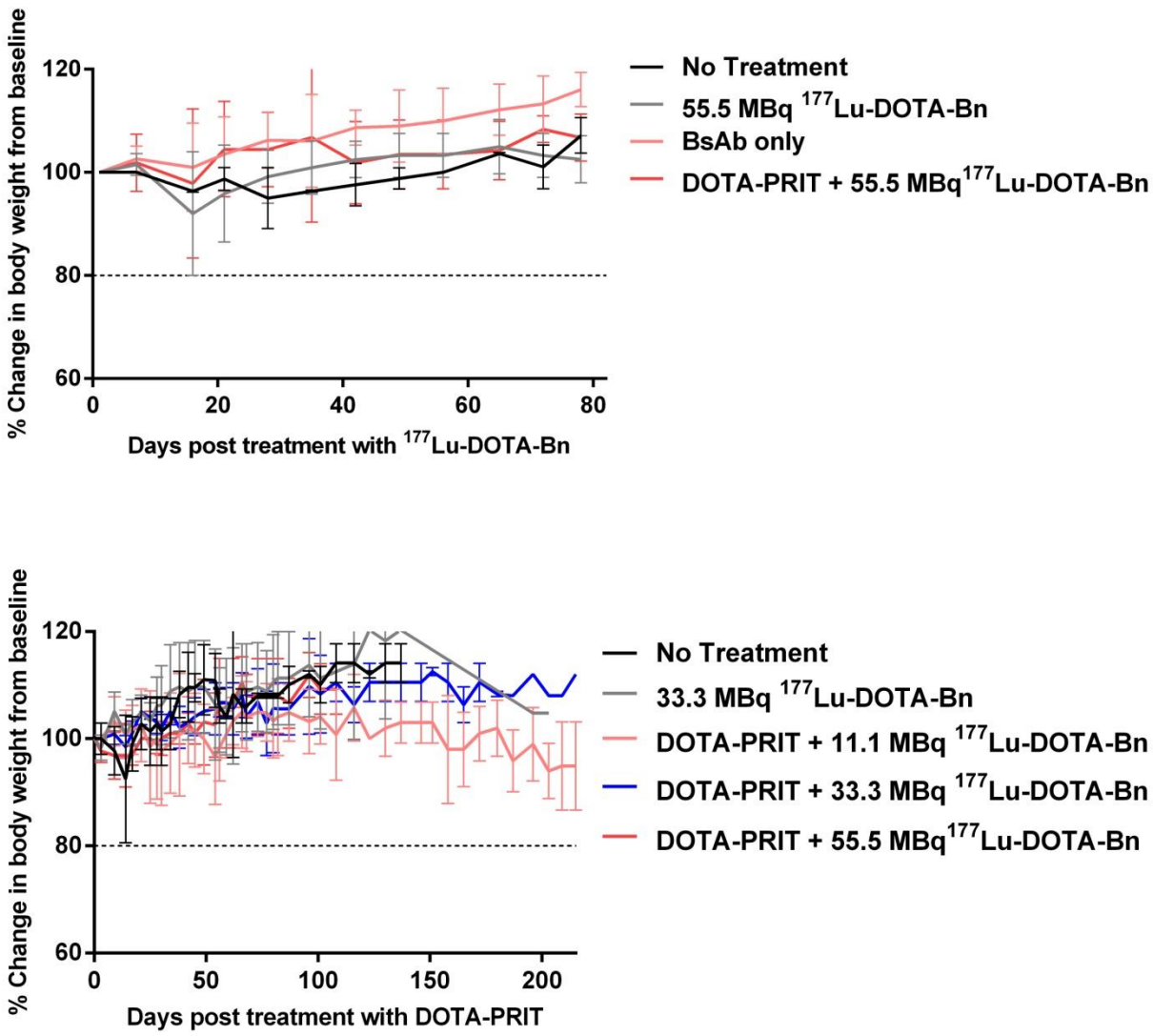


**Figure S5.** Animal weights at pre-treatment (baseline, day 0) up to ~85-200 d post-treatment with single-cycle anti-HER2-DOTA-PRIT + 11.1-55.5 MBq $^{177}$Lu-DOTA-Bn. Data is presented as mean ± SD.

**Table S5.** The number of animals taken out of the experiment based on predefined criteria of weight loss and tumor growth for single-cycle anti-HER2-DOTA-PRIT + 55.5 MBq of $^{177}$Lu-DOTA-Bn of groups of mice bearing small-sized tumors. The study endpoint was ~85 d post-treatment.

| Criteria to remove animal from experiment | No treatment | BsAb only | 55.5 MBq of $^{177}$Lu-DOTA-Bn only | DOTA-PRIT + 55.5 MBq of $^{177}$Lu-DOTA-Bn |
|---|---|---|---|---|
| Weight loss | 2/5 | 0/5 | 0/5 | 0/5 |
| Discovered deceased | 0/5 | 2/5 | 0/5 | 0/5 |
| Tumor burden | 0/5 | 0/5 | 0/5 | 0/5 |

Survivors at ~day 85: 3/5 from no treatment, 3/5 from BsAb only, 5/5 from 55.5 MBq of $^{177}$Lu-DOTA-Bn only, and 5/5 from anti-HER2-DOTA-PRIT + 55.5 MBq of $^{177}$Lu-DOTA-Bn

---

**Table S6.** The number of animals taken out of the experiment based on predefined criteria of weight loss and tumor growth for single-cycle anti-HER2-DOTA-PRIT + up to 55.5 MBq of $^{177}$Lu-DOTA-Bn of groups of mice bearing medium-sized tumors. The study endpoint was ~200 d post-treatment.

| Criteria to remove animal from experiment | No treatment | 33.3 MBq of $^{177}$Lu-DOTA-Bn only | DOTA-PRIT + 11.1 MBq of $^{177}$Lu-DOTA-Bn | DOTA-PRIT + 33.3 MBq of $^{177}$Lu-DOTA-Bn | DOTA-PRIT + 55.5 MBq of $^{177}$Lu-DOTA-Bn |
|---|---|---|---|---|---|
| Weight loss | 2/5 | 0/5 | 0/5 | 1/5 | 0/5 |
| Discovered deceased | 0/5 | 1/5 | 1/5 | 0/5 | 1/5 |
| Tumor burden | 3/5 | 4/5 | 0/5 | 3/5 | 3/5 |

Survivors at ~day 200: 4/5 from DOTA-PRIT + 11.1 MBq of $^{177}$Lu-DOTA-Bn, 1/5 each from DOTA-PRIT + 33.3 MBq of $^{177}$Lu-DOTA-Bn and DOTA-PRIT + 55.5 MBq of $^{177}$Lu-DOTA-Bn

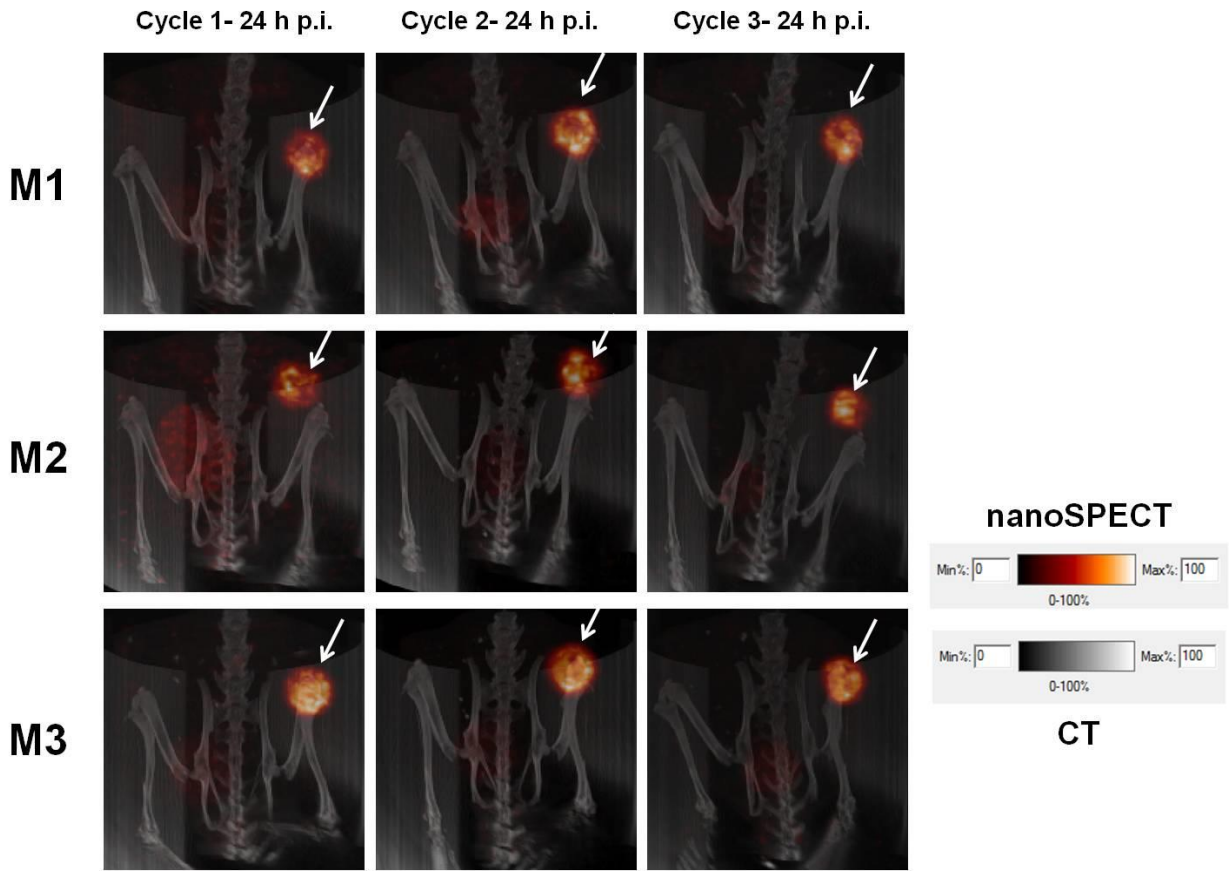


**Figure S6.** Theranostic fractionated anti-HER2-DOTA-PRIT + $^{177}$Lu-DOTA-Bn. SPECT/CT images (MIPs) of 3/8 animals (s.c. BT-474 tumors; randomly selected animals mouse 1 (M1), M2, and M3) undergoing fractionated three-cycle treatment with anti-HER2-DOTA-PRIT + 55.5 MBq of $^{177}$Lu-DOTA-Bn. White arrows indicate tumor in lower flank.

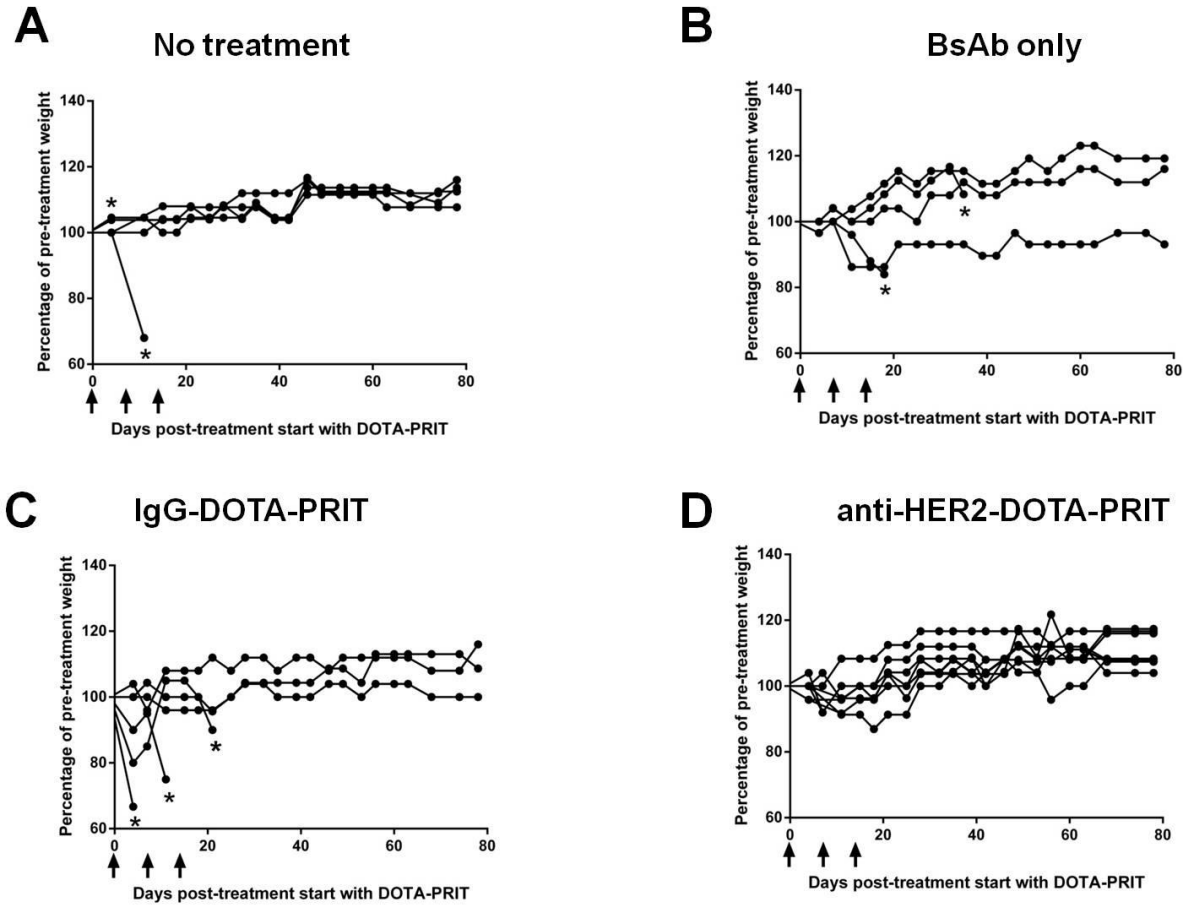


**Figure S7.** Animal weights at pre-treatment (baseline, day 0) up to 80 d post-treatment with treatment controls (A-C) or (D) fractionated anti-HER2-DOTA-PRIT. Black arrows indicate days of injection of $^{177}$Lu-DOTA-Bn. An asterisk denotes day of euthanasia due to excessive weight loss (i.e., when weight drops to 80% of baseline) *or* day when discovered deceased.

**Table S7.** The number of animals taken out of the experiment based on predefined criteria of weight loss and tumor growth for fractionated anti-HER2-DOTA-PRIT, study endpoint ~85 d post-treatment start.

| Criteria to remove animal from experiment | No treatment | BsAb only | Control IgG-DOTA-PRIT + $^{177}$Lu-DOTA-Bn | anti-HER2-DOTA-PRIT + $^{177}$Lu-DOTA-Bn |
|---|---|---|---|---|
| Weight loss | 1/6 | 1/5 | 3/6 | 0/8 |
| Discovered deceased | 1/6 | 1/5 | 0/6 | 0/8 |
| Tumor burden | 0/6 | 0/5 | 0/6 | 0/8 |

Survivors at ~day 85 included: 4/6 no treatment, 3/5 from BsAb only, 3/6 from IgG-DOTA-PRIT + $^{177}$Lu-DOTA-Bn and 8/8 from anti-HER2-DOTA-PRIT + $^{177}$Lu-DOTA-Bn.

Notes: Three animals from control groups that showed rapid deterioration of health and significant weight loss within 12-22 d of treatment start were submitted for necropsy to determine the cause of toxicity.

A single no-treated mouse showed rapid weight loss from pre-treatment weight at 12 d, and was submitted moribund for necropsy, while another non-treated control mouse was found dead at 18 d. The moribund animal had mild focal unilateral suppurative pyelonephritis with intralesional coccoid bacteria.

A single mouse from the BsAb only group showed rapid weight loss and was submitted for necropsy moribund at 20 d. This mouse showed pyelitis (bilateral) and pyelonephritis (unilateral), neutrophilic with intralesional bacteria (large cocci). A second mouse from the BsAb only group was discovered deceased at 35 d.

For treatment with Control IgG-DOTA-PRIT, three animals showed rapid weight loss from pre-treatment weight at 4, 11, and 21 d. A single mouse from this group was submitted moribund for necropsy at 22 d. This mouse was diagnosed with severe hypoplastic (aplastic) anemia and hypoplasia of growth plates in long bones with inanition, perimortem bacterial embolization, and perimortem hemorrhage.

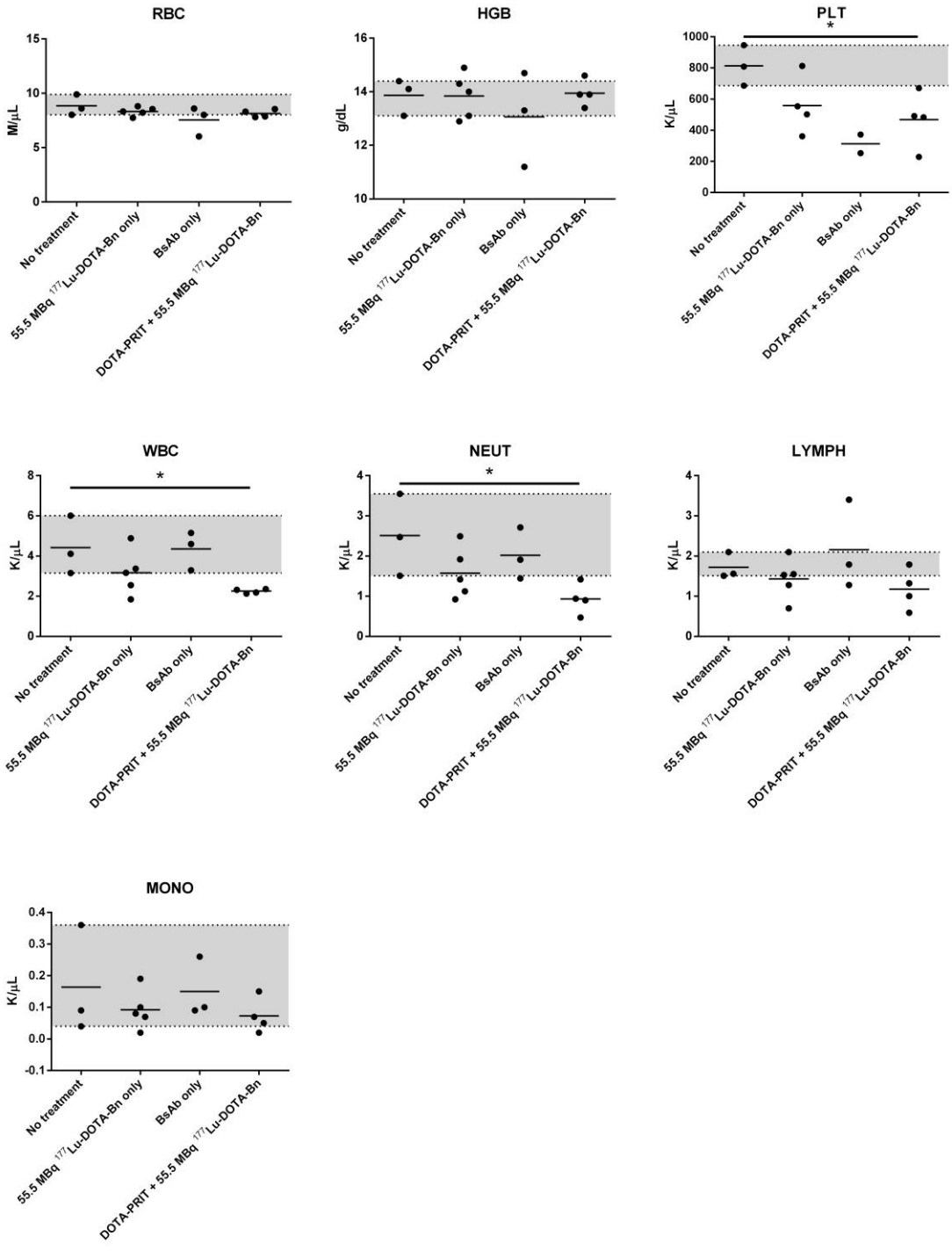


**Figure S8.** Hematology values at ~85 d from s.c. BT-474 tumor-bearing mice (smaller tumors) that underwent single-cycle anti-HER2-DOTA-PRIT + 55.5 MBq $^{177}$Lu-DOTA-Bn. RBC: red blood cells, HGB: hemoglobin, PLT: platelets, WBC: white blood cells, NEUT: neutrophils, LYMPH: lymphocytes, MONO: monocytes. Notes: Two animals showed low values for PLT: a mouse treated with 55.5 MBq $^{177}$Lu-DOTA-Bn only (PLT: 57) and one treated with BsAb only (PLT: 0); since platelet clumps were noted, values were excluded from analysis and considered an artifact of blood sampling. *$P$ < 0.05

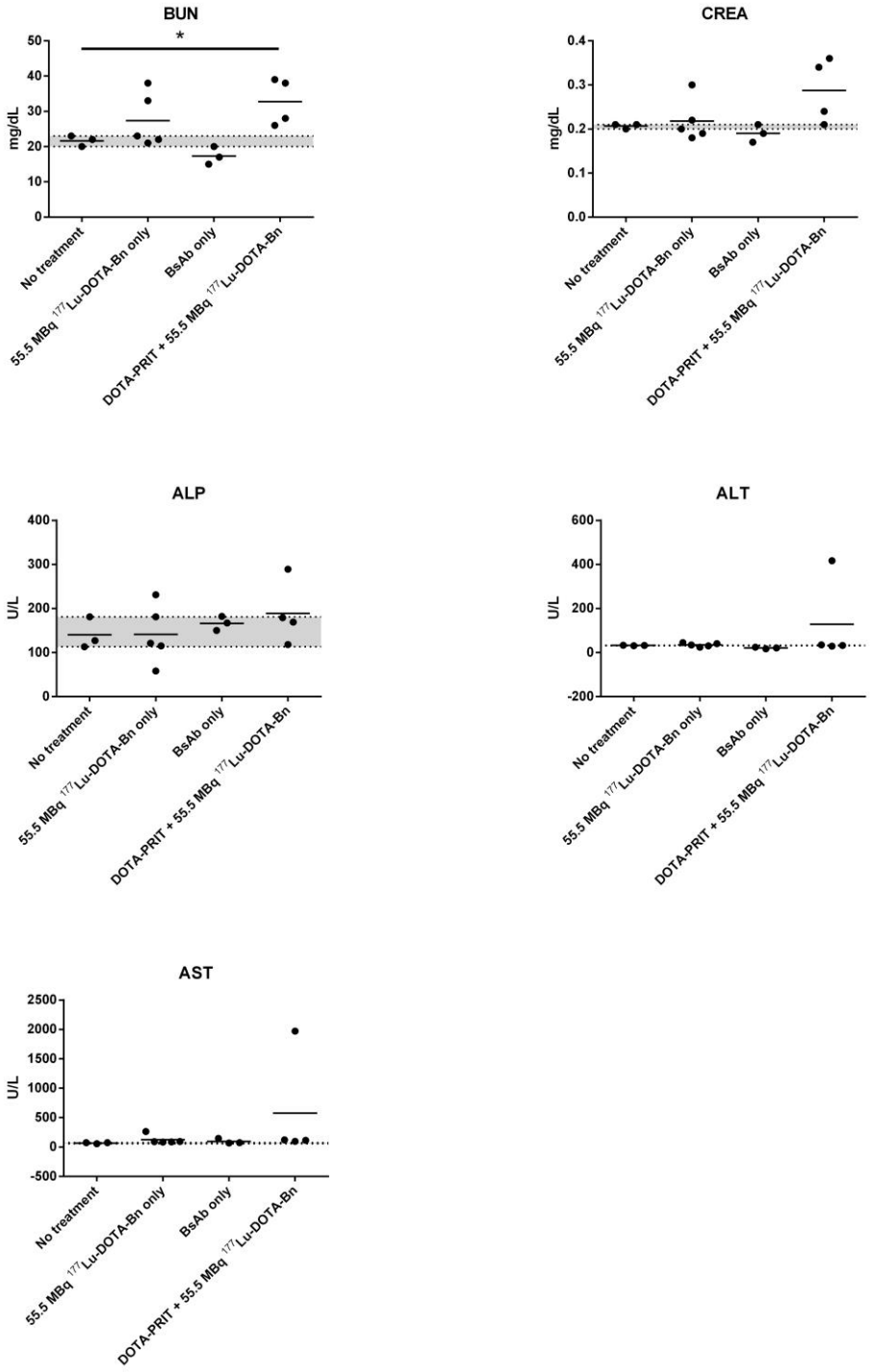


**Figure S9.** Clinical chemistry values at ~85 d from s.c. BT-474 tumor-bearing mice (smaller tumors) that underwent single-cycle anti-HER2-DOTA-PRIT + 55.5 MBq $^{177}$Lu-DOTA-Bn. BUN: blood urea nitrogen, CREA: creatinine, ALP: alanine phosphatase, ALT: alanine aminotransferase, AST: aspartate aminotransferase. *$P$ < 0.05

**Table S8.** Histopathologic findings at ~85 d post-treatment from BT-474 tumor-bearing mice (smaller tumors) that underwent single-cycle anti-HER2-DOTA-PRIT + $^{177}$Lu-DOTA-Bn. A total of 15 animals were evaluated by necropsy.

| | No treatment | | | 55.5 MBq of $^{177}$Lu-DOTA-Bn only | | | | |
|---|---|---|---|---|---|---|---|---|
| Tumor | 12 x 6 x 3 mm; AC with necrosis and L inflammation, 3 | 7 x 6 x 2 mm; AC | Two lesions: 15 x 10 x 9 mm and 5 x 5 x 5 mm; AC, with necrosis | Two lesions: 5 x 5 x 2 mm and 2 x 2 x 2 mm AC, with L inflammation, 3 | 14 x 10 x 4 mm; AC, with L inflammation, 3 | 16 x 16 x 6 mm; AC, with necrosis and L inflammation, 2 | 6 x 6 x 2 mm; AC | 9 x 7 x 3 mm; AC |
| Liver | Hepatitis, L, portal, MF, 1 | Hepatitis, L, portal, MF, 2. EM, 2 | Hepatitis, L, portal, MF, 1 | Hepatitis, L, portal, MF, 2. EM, 1 | Hepatitis, L, portal, MF, 1 | N | Hepatitis, L, portal, MF, 2 | Hepatitis, L, portal, MF, 1 |
| Kidney | Tubular degeneration, 2, MF, bilateral | Tubular degeneration, 2, MF, bilateral | N | N | N | Tubular degeneration, 1, focal, unilateral | Tubular degeneration, 1, focal, unilateral | (Left): MF cortical and medullary atrophy and fibrosis, chronic (consistent with multiple chronic infarcts, or chronic resolved pyelonephritis); (Right): pyelonephritis, 3, neutrophilic, with bacteria (cocci), subacute |
| Spleen | LH and plasmacytosis, 2 | LH, 2. EM, 3. | N | Plasmacytosis, 3 | LH and plasmacytosis, 2 | HH, 3 | N | N |
| Bones | FL | FL | FL | FL | FL | FL | FL | FL |
| Bone marrow | N | MH | MH | MH | N | MH | N | MH |

AC: Anaplastic carcinoma, L: Lymphoplasmacytic, N: Normal, EM: Extramedullary hematopoiesis, HH: Hematopoietic hyperplasia, LH: Lymphoid hyperplasia, FE: Focally extensive, FL: Fibro-osseous lesions, MH: Myeloid hyperplasia, MF: Multifocal, MFR: Multifocal random, 1: Minimal, 2: Mild, 3: Moderate, 4: Marked

**Table S8, continued.**

| | BsAb only | | | anti-HER2-DOTA-PRIT + 55.5 MBq | | | |
|---|---|---|---|---|---|---|---|
| Tumor | No tumor | 5 x 5 x 3 mm; AC, with lymphocytic inflammation, 2 | 13 x 9 x 4 mm; AC, with necrosis and lymphocytic inflammation, 1 | 3 x 3 x 2 mm and 2 x 2 x 2 mm; AC | 2 x 2 x 2 mm; no evidence of neoplasia | FE area of fibrosis in subcutis. No evidence of neoplasia. Overlying epidermis shows acanthosis and hyperkeratosis, 3 | 3 x 2 x 1 mm; no evidence of neoplasia. Overlying epidermis shows acanthosis and hyperkeratosis, 3 |
| Liver | Hepatitis, L, portal, MF, 1 | Hepatitis, L, portal, MF, 1 | N | Hepatitis, L, portal, MF, 1 | Hepatitis, L, portal, MF, 1. EM, 1 | Hepatitis, L, portal, MF, 1 | N |
| Kidney | Tubular degeneration, 1, MF, bilateral | N | N | N | Unilateral hydronephrosis, 3 | N | N |
| Spleen | LH, 2 | EM, 3 | N | LH, 2 | N | N | LH and plasmacytosis, 2 |
| Bones | N | FL | FL | FL | FL | FL | FL |
| Bone marrow | N | N | MH | N | MH | N | N |

AC: Anaplastic carcinoma, L: Lymphoplasmacytic, N: Normal, EM: Extramedullary hematopoiesis, HH: Hematopoietic hyperplasia, LH: Lymphoid hyperplasia, FE: Focally extensive, FL: Fibro-osseous lesions, MH: Myeloid hyperplasia, MF: Multifocal, MFR: Multifocal random, 1: Minimal, 2: Mild, 3: Moderate, 4: Marked

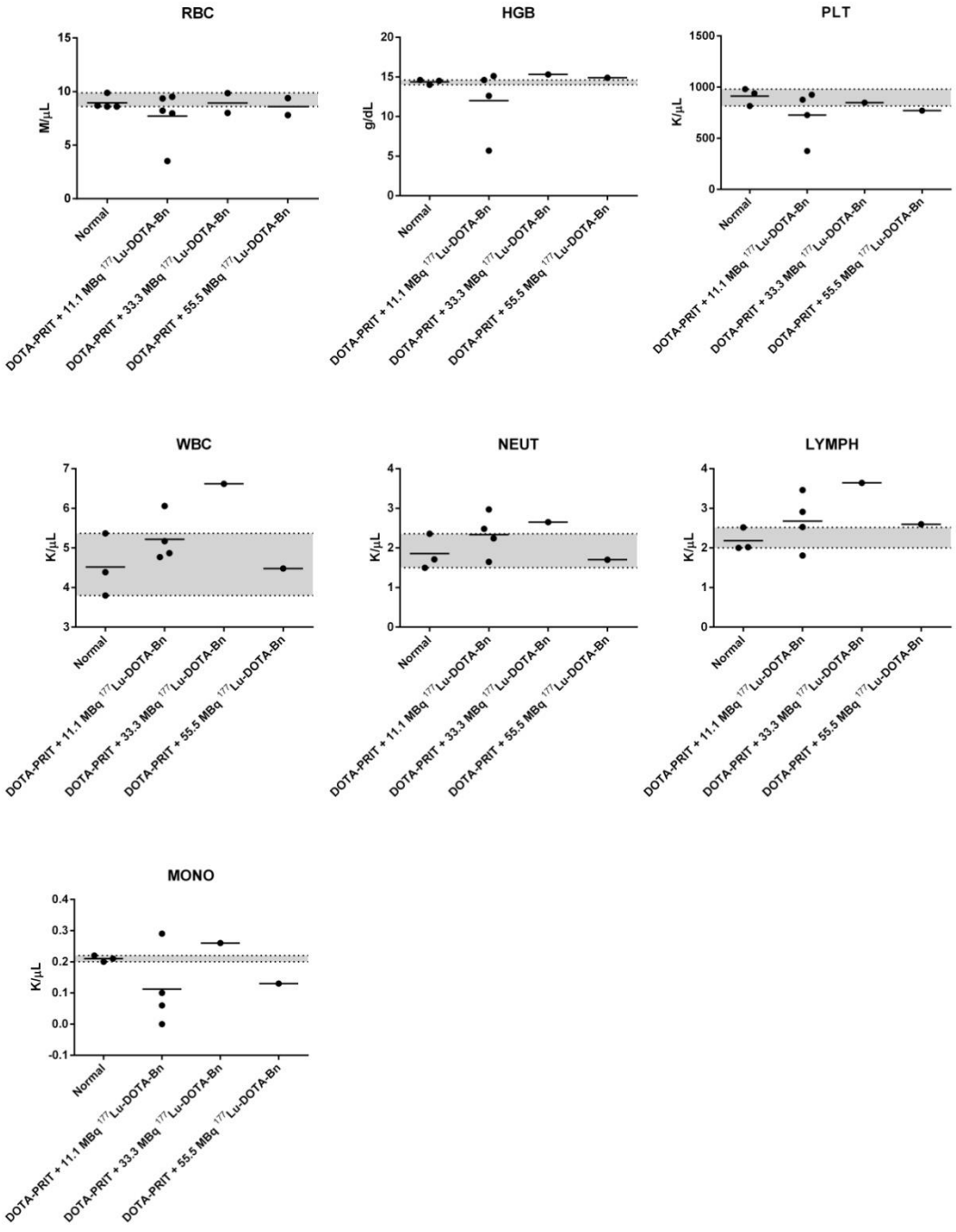


**Figure S10.** Hematology values at ~200 d from BT-474 tumor-bearing mice (medium-sized tumors) that underwent single-cycle DOTA-PRIT + $^{177}$Lu-DOTA-Bn. Due to the small number of survivors at 200 d and lack of untreated controls, no statistical comparisons between groups were made. RBC: red blood cells, HGB: hemoglobin, PLT: platelets, WBC: white blood cells, NEUT: neutrophils, LYMPH: lymphocytes, MONO: monocytes. Normal animals: Harlan, Athymic Nude, Hsd:Athymic Nude-Foxn1$^{nu}$, ~3 month old females, with no estrogen or xenograft implanted.

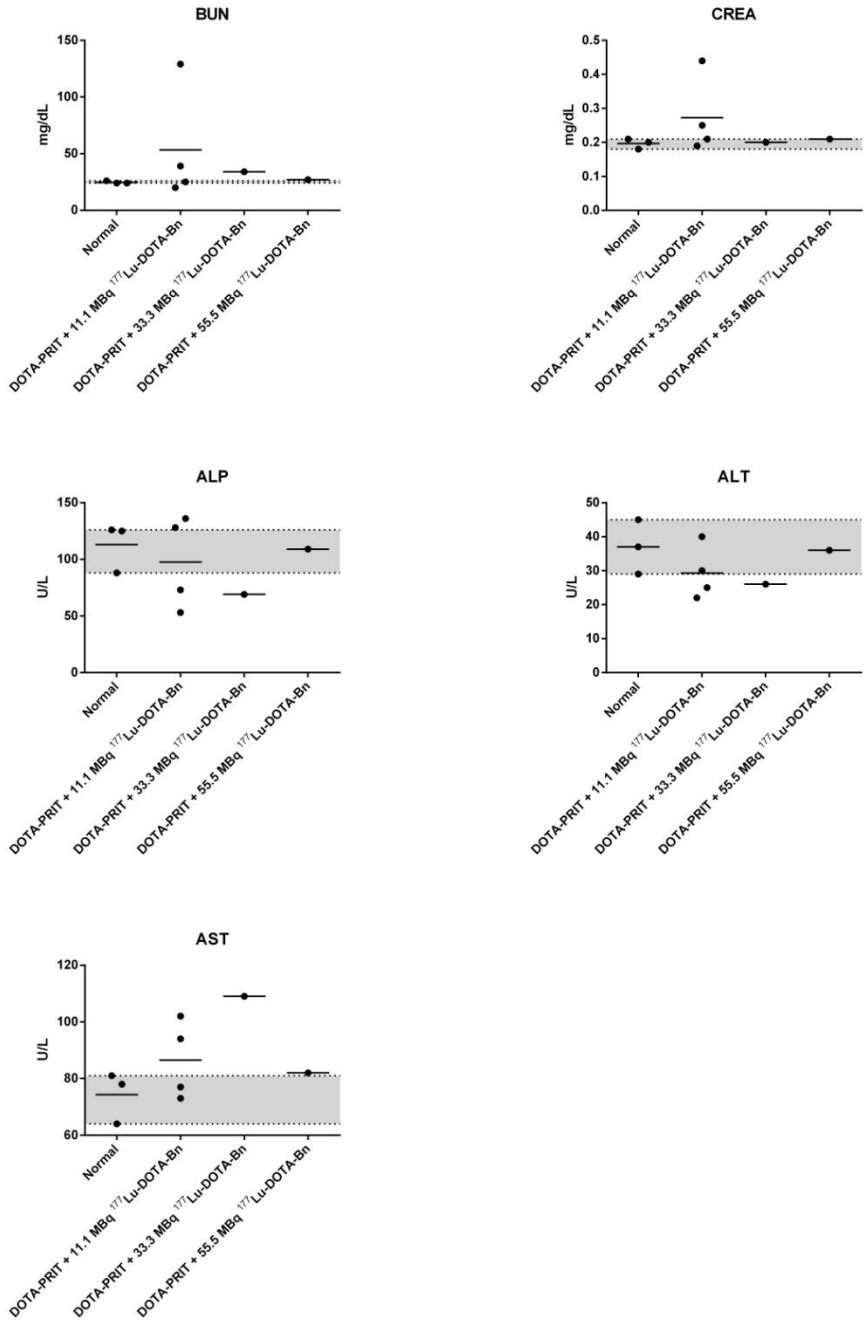


**Figure S11.** Clinical chemistry values at ~200 d from BT-474 tumor-bearing mice (medium-sized tumors) that underwent single-cycle anti-HER2-DOTA-PRIT + $^{177}$Lu-DOTA-Bn. Due to the small number of survivors at 200 d and lack of untreated controls, no statistical comparisons between groups were made. BUN: blood urea nitrogen, CREA: creatinine, ALP: alanine phosphatase, ALT: alanine aminotransferase, AST: aspartate aminotransferase. Normal animals: Harlan, Athymic Nude, Hsd:Athymic Nude-Foxn1$^{nu}$, ~3 month old females, with no estrogen or xenograft implanted.

**Table S9.** Histopathologic findings at ~200 d post-treatment from BT-474 tumor-bearing mice (medium-sized tumors) that underwent single-cycle anti-HER2-DOTA-PRIT + $^{177}$Lu-DOTA-Bn. A total of 6 animals were evaluated by necropsy.

| | DOTA-PRIT + 11.1 MBq | | | | DOTA-PRIT + 33.3 MBq | DOTA-PRIT + 55.5 MBq |
|---|---|---|---|---|---|---|
| Tumor | FE fibrosis with minimal L and histiocytic inflammation; no evidence of neoplasia | 15 x 10 x 6 mm; poorly demarcated and invasive neoplasm composed of epithelioid cells forming nests with an abundant fibrous stroma. MF necrosis and calcification. Lymphocytic inflammation within tumor, 2, MF. Evidence of vascular invasion. Overlying epidermis shows moderate acanthosis and hyperkeratosis | 20 x 15 x 12 mm; AC, with necrosis, lymphocytic inflammation 2, and vascular invasion. Overlying epidermis shows acanthosis, 3, and hyperkeratosis | 10 x 6 x 2 mm; poorly demarcated and invasive neoplasm. MF necrosis and MF lymphocytic inflammation, 3. Overlying epidermis shows moderate acanthosis and hyperkeratosis | 10 x 5 x 5 mm; poorly demarcated and invasive neoplasm. MF necrosis and MF lymphocytic inflammation, 1. Overlying epidermis shows moderate acanthosis and hyperkeratosis | 3 x 3 x 1 mm; FE fibrosis with L inflammation, 1; no evidence of neoplasia. Overlying epidermis shows acanthosis, 3, and hyperkeratosis |
| Liver | Hepatitis, L and neutrophilic, 1, MFR. EM, 1 | Hepatitis, L, portal, MF, 1 | Hepatitis, L, portal, MF, 1 | Hepatitis, L, random, MF, 2 | Hepatitis, L, portal, MF, 2 | Hepatitis, L, portal, MF, 1 |
| Kidney | (Left): Pyelonephritis, neutrophilic, with bacteria (bacilli), chronic-active, 4. Membranous glomerulonephritis, MF, chronic, 4; (Right): Pyelonephritis, neutrophilic, with bacteria, subacute, 3. Membranous glomerulonephritis, MF, with tubular hyaline casts and degeneration, chronic, 4 | Tubular degeneration, MF, bilateral, 2. (Left): Pyelitis, neutrophilic, acute, 2. Metastatic AC; (Right) L, MF, with diffuse atrophy, 4, and fibrosis, chronic, 3 | Metastatic AC. Tubular degeneration, 2, necrosis, and loss, MF, bilateral | N | N | N |
| Spleen | HH, 3 | N | LH, 2 | LH, 2 | LH, 2 | LH, 2 |
| Bones | MH | N | N | N | N | N |

AC: Anaplastic carcinoma, L: Lymphoplasmacytic, N: Normal, EM: Extramedullary hematopoiesis, HH: Hematopoietic hyperplasia, LH: Lymphoid hyperplasia, FE: Focally extensive, FL: Fibro-osseous lesions, MH: Myeloid hyperplasia, MF: Multifocal, MFR: Multifocal random, 1: Minimal, 2: Mild, 3: Moderate, 4: Marked

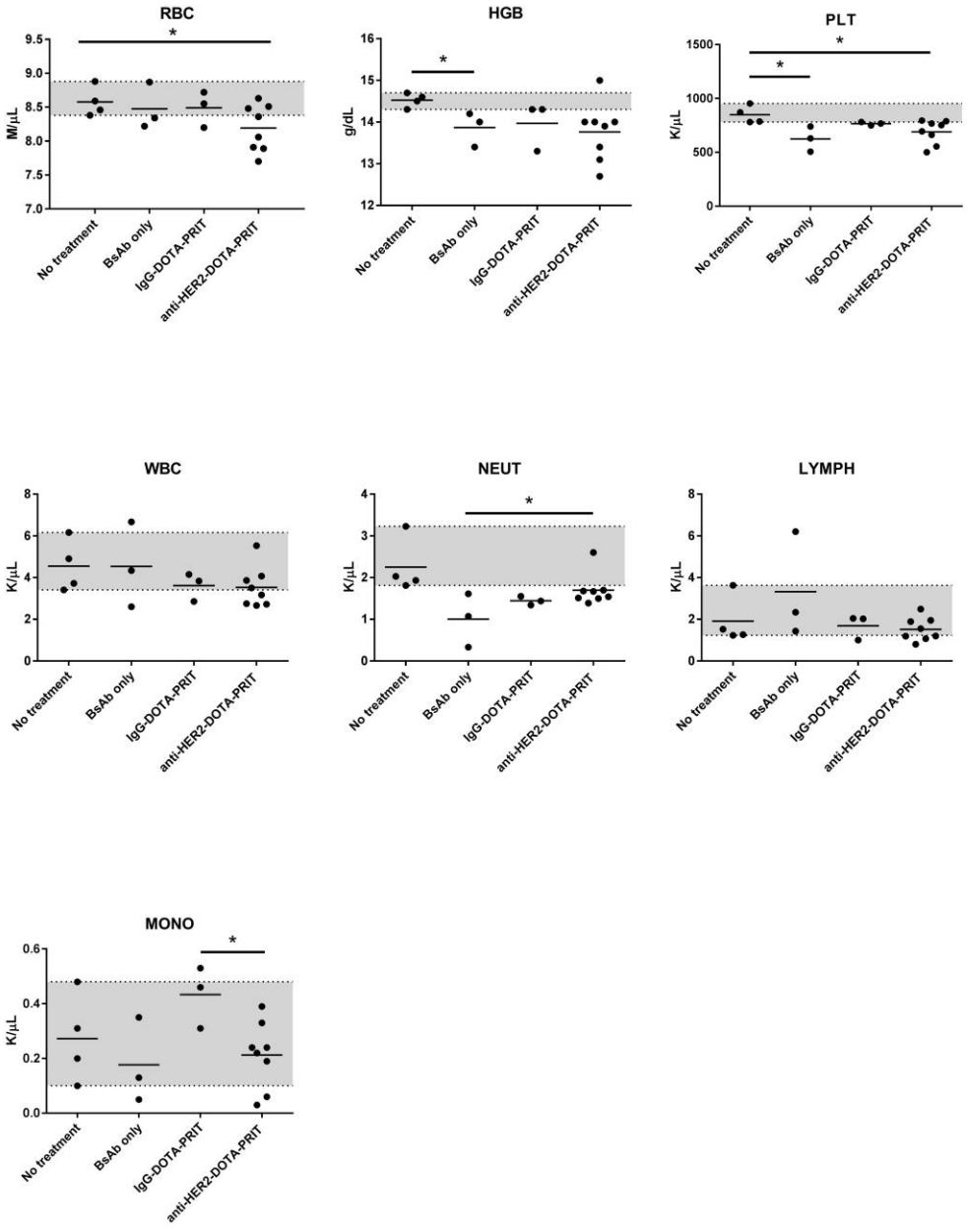


**Figure S12.** Hematology values at ~85 d post-treatment start from BT-474 tumor-bearing mice (medium-sized tumors) that underwent fractionated Control IgG-DOTA-PRIT or anti-HER2-DOTA-PRIT with $^{177}$Lu-DOTA-Bn (167 MBq/mouse total administered activity). RBC: red blood cells, HGB: hemoglobin, PLT: platelets, WBC: white blood cells, NEUT: neutrophils, LYMPH: lymphocytes, MONO: monocytes. *$P$ < 0.05.

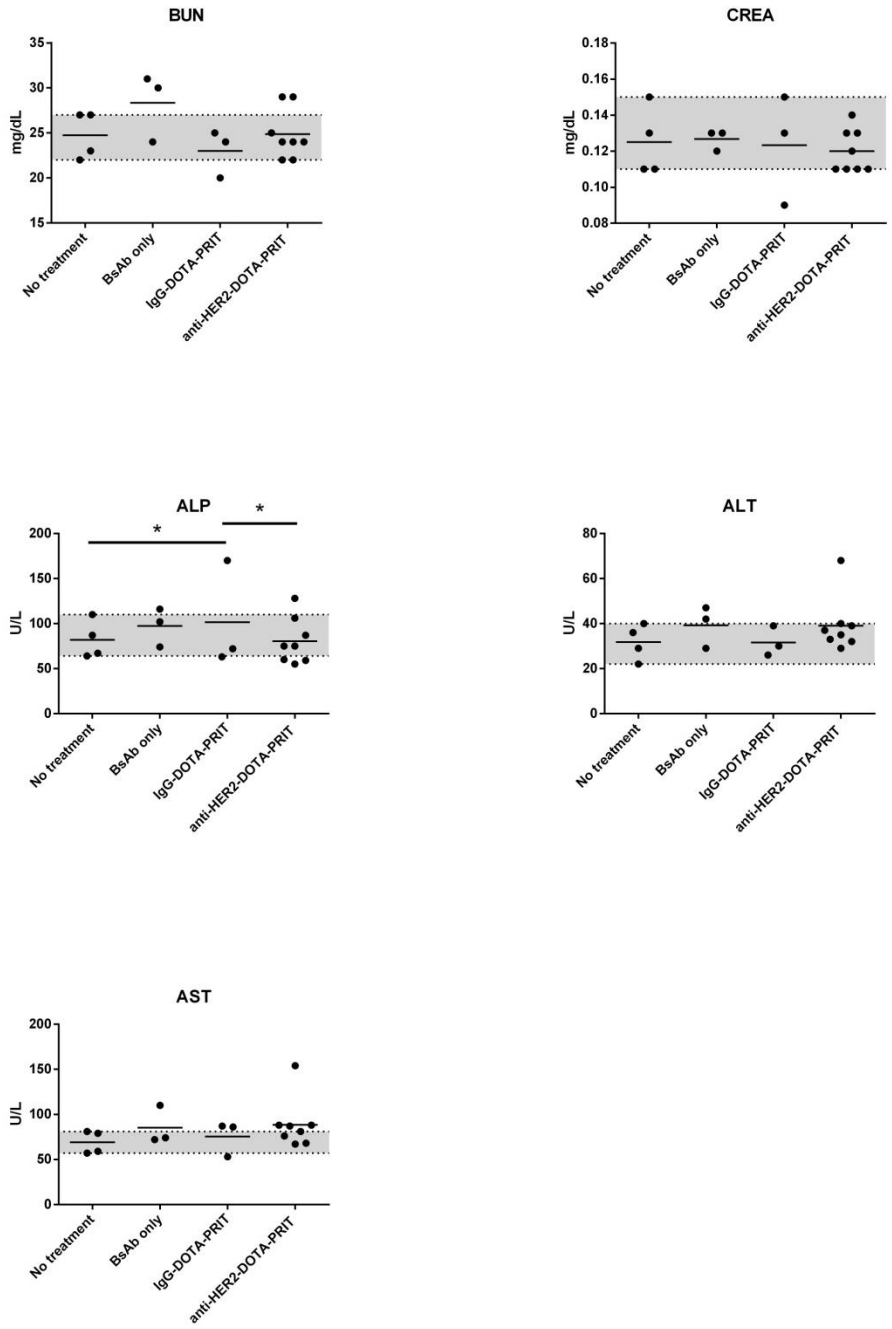


**Figure S13.** Clinical chemistry values at ~85 d post-treatment start from BT-474 tumor-bearing mice (medium-sized tumors) that underwent fractionated Control IgG-DOTA-PRIT or anti-HER2-DOTA-PRIT with $^{177}$Lu-DOTA-Bn (167 MBq/mouse). BUN: blood urea nitrogen, CREA: creatinine, ALP: alanine phosphatase, ALT: alanine aminotransferase, AST: aspartate aminotransferase. *$P$ < 0.05.

**Table S10.** Histopathologic findings at ~85 d from BT-474 tumor-bearing mice (medium-sized tumors) that underwent fractionated anti-HER2-DOTA-PRIT + $^{177}$Lu-DOTA-Bn. A total of 18 animals were evaluated by necropsy.

| | No treatment | | | | BsAb only | | |
|---|---|---|---|---|---|---|---|
| Tumor | 15 x 12 x 5 mm; AC | 15 x 10 x 5 mm; AC | 14 x 12 x 2 mm; AC | 2 coalescing round nodules on right flank. 7 mm in diameter and 5 mm thick | 10 x 15 x 3 mm; AC | 20 x 17 x 7 mm; AC. Increased infiltration of lymphocytes and plasma cells within subcutis immediately surrounding the mass, even forming follicular-like structures | 12 x 12 x 6 mm; AC |
| Liver | Occasional small foci (few scattered cells) of periportal lymphocytes and plasma cells | N | Focal basophilic focus with hepatocellular hypertrophy | Diffuse hepatocellular polyploidia and karyomegaly | N | N | L infiltrate within portal fields, 1 |
| Kidney | N | Unilateral focal minimal hyaline casts within medullary tubules | N | N | Within the cortex MF segmental basophilia | N | N |
| Spleen | N | N | Slightly increased EH and hemosiderosis | EH, 2-3 | White pulp hyperplasia (reactive) | Increase of EH, 2 | Hemosid erosis, 1 |
| Bone marrow | N | MF myelofibrosis, 2 | Slightly decreased erythroid elements | Mild decrease of erythroid precursors density | MF myelofibrosis and slightly decreased erythroid precursors in stifle only | N | FM in stifle |

AC: Anaplastic carcinoma, L: Lymphoplasmacytic, N: Normal, EM: Extramedullary hematopoiesis, HH: Hematopoietic hyperplasia, LH: Lymphoid hyperplasia, FE: Focally extensive, FL: Fibro-osseous lesions, FM: Focal myelofibrosis, MH: Myeloid hyperplasia, MF: Multifocal, MFR: Multifocal random, 1: Minimal, 2: Mild, 3: Moderate, 4: Marked

**Table S10, continued.**

| | Control IgG-DOTA-PRIT + $^{177}$Lu-DOTA-Bn | | | anti-HER2-DOTA-PRIT + $^{177}$Lu-DOTA-Bn | | | | | | | |
|---|---|---|---|---|---|---|---|---|---|---|---|
| Tumor | AC, firm in texture, 0.5 x 0.5 x 0.1 cm. Tumor mass extends from subcutis into skeletal muscle | AC, 1.5 x 1.2 x 0.8 cm; texture is firm to hard | AC, 1 x 1 x 0.5 cm. Tumor extends from subcutis into fascia | No mass along flank. Subcutis is focally expanded by abundant collagen with few fibroblasts (sclerosis). Only few single neoplastic cells were found, scattered within extracellular matrix | No mass along flank. Site consists of sclerotic stroma, with no evidence of neoplastic cells in section. | No mass along flank. Site consists of sclerotic tissue, with no evidence of neoplastic cells in section | No mass along flank. Dermis and subcutis are replaced by sclerotic collagen. No neoplastic cells were found in examined section | A single round mass, 0.3 cm diameter, 0.2 cm thick. Mass consists of sclerotic stroma in which few scattered neoplastic cells are embedded | A single round mass along right flank, 0.3 cm diameter, 0.2 cm thick. Mass consists of sclerotic stroma. No neoplastic cells | No mass along flank. Site consists of focal sclerosis with few scattered neoplastic cells | No mass along flank. No evidence of neoplastic cells in section |
| Liver | N | N | Minimal and focal hepatocellular necrosis. Mild infiltration of lymphocytes and plasma cells within portal spaces | N | N | N | N | MF hepatocellular hypertrophy and acidophilia. L portal infiltration, 1 | N | L infiltration of the portal triads, 2 | N |
| Kidney | N | N | N | N | N | N | N | N | N | N | N |
| Spleen | Increase of EH (erythroid line), 3 | Increase of EH (erythroid line), 3 to severe | N | Increase of EH (erythroid line), 2 | N | N | EH, 2-3 | EH, 3 | N | EH, 2 | EH, 2-3 |
| Bone marrow | N | Ratio between erythroid and myeloid components is equivalent (normal 1:3). Erythroid compartment is depleted of both mature and immature forms | N | MF myelofibrosis and slightly decreased erythroid precursors in stifle only | N | Decrease erythroid line elements in vertebras only | FM in stifle, 2 | FM with decreased erythroid elements | N | N | FM in stifle |

AC: Anaplastic carcinoma, L: Lymphoplasmacytic, N: Normal, EM: Extramedullary hematopoiesis, HH: Hematopoietic hyperplasia, LH: Lymphoid hyperplasia, FE: Focally extensive, FL: Fibro-osseous lesions, FM: Focal myelofibrosis, MH: Myeloid hyperplasia, MF: Multifocal, MFR: Multifocal random, 1: Minimal, 2: Mild, 3: Moderate, 4: Marked

**Table S11.** Pathology severity scoring of remarkable morphological changes. Summary of distribution and incidence of morphologic changes in the different groups at ~85 d post-treatment start from groups that underwent fractionated DOTA-PRIT + $^{177}$Lu-DOTA-Bn. Treatment groups included: No treatment, BsAb only (BsAb), Control IgG-DOTA-PRIT + $^{177}$Lu-DOTA-Bn (IgG-therapy), and anti-HER2-DOTA-PRIT + $^{177}$Lu-DOTA-Bn (anti-HER2-therapy).

| Organ | Morphologic change | % Incidence (No. mice with lesions/No. mice examined) | | | | Score* | | | |
|---|---|---|---|---|---|---|---|---|---|
| | | No treatment | BsAb only | Control IgG-therapy | anti-HER2-therapy | No treatment | BsAb | Control IgG-therapy | anti-HER2-therapy |
| Kidney | Unilateral focal presence of hyaline casts in medullary tubules | 25 (1/4) | 0 (0/3) | 0 (0/3) | 0 (0/8) | 2 | 0 | 0 | 0 |
| | Unilateral, multifocal, cortical tubular basophilia | 0 (0/4) | 33.3 (1/3) | 0 (0/3) | 0 (0/8) | 0 | 3 | 0 | 0 |
| Total organ severity score | | | | | | 2 | 3 | 0 | 0 |
| Spleen | Extramedullary hematopoiesis, 2 | 0 (0/4) | 33.3 (1/3) | 0 (0/3) | 25 (2/8) | 0 | 2 | 0 | 2 |
| | 2-3 | 25 (1/4) | 0 (0/3) | 0 (0/3) | 25 (2/8) | 2.5 | 0 | 0 | 2.5 |
| | 3 | 0 (0/4) | 0 (0/3) | 33.3 (1/3) | 12.5 (1/8) | 0 | 0 | 3 | 3 |
| | 3-4 | 0 (0/4) | 0 (0/3) | 33.3 (1/3) | 0 (0/8) | 0 | 0 | 3.5 | 0 |
| Total organ severity score | | | | | | 2.5 | 2 | 6.5 | 7.5 |
| Bone marrow | Multifocal myelofibrosis | 25 (1/4) | 0 (0/3) | 0 (0/3) | 0 (0/8) | 2 | 0 | 0 | 0 |
| | Diffuse myelofibrosis | 0 (0/4) | 0 (0/3) | 0 (0/3) | 0 (0/8) | 0 | 0 | 0 | 0 |
| | Focal myelofibrosis | 0 (0/4) | 33.3 (1/3) | 0 (0/3) | 12.5 (1/8) | 0 | 1 | 0 | 1 |
| | Erythroid compartment is depleted of both mature and immature forms | 0 (0/4) | 0 (0/3) | 33.3 (1/3) | 0 (0/8) | 0 | 0 | 3 | 0 |
| Total organ severity score | | | | | | 2 | 1 | 3 | 1 |

**Please see **Table S12** for scoring.*

**Table S12**. Calculation of organ severity scores described in Table S11.

| Extension | Score | Distribution (for paired organs) | Score |
|---|---|---|---|
| Focal | 1 | Single organ | 0 |
| Multifocal | 2 | Unilateral | 1 |
| Diffuse | 3 | Bilateral | 2 |

Severity scoring system of histopathologic lesions:

Total scoring formula: Extension score + Distribution score

Total severity per organ: Sum of partial scores for single histopathologic lesions